



HAL
open science

Organ-specific quality control of plant peroxisomes is mediated by autophagy

Koki Yoshimoto, Michitaro Shibata, Maki Kondo, Kazusato Oikawa, Mayuko Sato, Kiminori Toyooka, Ken Shirasu, Mikio Nishimura, Yoshinori Ohsumi

► **To cite this version:**

Koki Yoshimoto, Michitaro Shibata, Maki Kondo, Kazusato Oikawa, Mayuko Sato, et al.. Organ-specific quality control of plant peroxisomes is mediated by autophagy. *Journal of Cell Science*, 2014, 127 (6), pp.1161-1168. 10.1242/jcs.139709 . hal-01204043

HAL Id: hal-01204043

<https://hal.science/hal-01204043>

Submitted on 28 May 2020

HAL is a multi-disciplinary open access archive for the deposit and dissemination of scientific research documents, whether they are published or not. The documents may come from teaching and research institutions in France or abroad, or from public or private research centers.

L'archive ouverte pluridisciplinaire **HAL**, est destinée au dépôt et à la diffusion de documents scientifiques de niveau recherche, publiés ou non, émanant des établissements d'enseignement et de recherche français ou étrangers, des laboratoires publics ou privés.

SHORT REPORT

Organ-specific quality control of plant peroxisomes is mediated by autophagy

Kohki Yoshimoto^{1,2,3,‡}, Michitaro Shibata^{4,5}, Maki Kondo⁴, Kazusato Oikawa^{4,*}, Mayuko Sato^{1,6}, Kiminori Toyooka^{1,6}, Ken Shirasu^{1,6}, Mikio Nishimura^{4,5} and Yoshinori Ohsumi^{7,‡}

ABSTRACT

Peroxisomes are essential organelles that are characterized by the possession of enzymes that produce hydrogen peroxide (H₂O₂) as part of their normal catalytic cycle. During the metabolic process, peroxisomal proteins are inevitably damaged by H₂O₂ and the integrity of the peroxisomes is impaired. Here, we show that autophagy, an intracellular process for vacuolar degradation, selectively degrades dysfunctional peroxisomes. Marked accumulation of peroxisomes was observed in the leaves but not roots of autophagy-related (*ATG*)-knockout *Arabidopsis thaliana* mutants. The peroxisomes in leaf cells contained markedly increased levels of catalase in an insoluble and inactive aggregate form. The chemically inducible complementation system in *ATG5*-knockout *Arabidopsis* provided the evidence that these accumulated peroxisomes were delivered to vacuoles for degradation by autophagy. Interestingly, autophagosomal membrane structures specifically recognized the abnormal peroxisomes at the site of the aggregates. Thus, autophagy is essential for the quality control of peroxisomes in leaves and for proper plant development under natural growth conditions.

KEY WORDS: Autophagy, Organelle degradation, Plant leaf, Quality control

INTRODUCTION

Peroxisomes are essential organelles characterized by the possession of enzymes that produce hydrogen peroxide (H₂O₂) as part of their normal catalytic cycle (De Duve and Baudhuin, 1966). In plant leaves, two major types of peroxisomes play crucial roles in the postgerminative development of seedlings and photosynthesis (Beevers, 1979). A type of plant peroxisome, the glyoxysome, is involved in fatty acid β-oxidation to convert storage oil into carbohydrates in cotyledons, the embryonic first

leaves, to support the postgerminative growth of seedlings until the commencement of photoautotrophic growth. The other prominent type of plant peroxisome, the leaf peroxisome, is unique in that it plays an important role in photorespiration (i.e. the photosynthesis-related oxidative carbon cycle). In both metabolic pathways, especially in photorespiration, H₂O₂ is generated by oxidative reactions (Foyer and Noctor, 2003) and is scavenged by catalase, which is present in both types of peroxisomes (del Río et al., 2006). Proteins in peroxisomes are damaged by reactive oxygen species (ROS) produced during such peroxisomal oxidation processes. Plants with impaired peroxisome function exhibit a defect in seedling development and have decelerated growth phenotypes (Reumann and Weber, 2006; Fulda et al., 2004; Rylott et al., 2006), indicating that the maintenance and turnover of peroxisomes are important for plant development and growth. Despite their importance, the mechanism by which the basal quality of peroxisomes is maintained is unknown.

Macroautophagy (referred to hereafter as autophagy) is an evolutionarily conserved intracellular process in eukaryotes, which involves the degradation of cytoplasmic constituents and organelles by sequestration in double-membraned vesicles, the autophagosomes (Mizushima et al., 2011). In yeast, phytopathogens and animal cells, there is a type of autophagy that is specific for peroxisome degradation, known as ‘pexophagy’. This involves the removal of excess or redundant peroxisomes under particular artificial growth conditions in which peroxisomal functions are no longer required (Sakai et al., 2006; Asakura et al., 2009; Iwata et al., 2006). However, the role of pexophagy in the quality control of peroxisomes remains obscure.

RESULTS AND DISCUSSION

We investigated the behavior of peroxisomes in *ATG*-knockout *Arabidopsis thaliana* (*atg* mutants) expressing green fluorescent protein (GFP) fused with PTS1 (Mano et al., 2002), a peroxisomal targeting signal. The number of peroxisomes was increased in the leaves of all *atg* mutants examined (Fig. 1A, upper-right panel; Fig. 1B; supplementary material Fig. S1A,B). By contrast, there was no obvious difference in the number of peroxisomes in roots between wild-type plants and *atg* mutants (Fig. 1A, lower panels; supplementary material Fig. S1C,D). Western blotting analysis using antibodies against the representative peroxisomal protein catalase further confirmed these imaging data. Although there were no substantial differences in the transcript levels of catalase genes (supplementary material Fig. S2A; Frugoli et al., 1996), the catalase protein levels were markedly increased in *atg5* leaves, but not in the roots, compared to wild-type controls (Fig. 1C). These results suggest that the number of photosynthesis-related peroxisomes is increased in *atg* mutants.

¹RIKEN Plant Science Center, Tsurumi-ku, Yokohama 230-0045, Japan. ²INRA, UMR1318, Institut Jean-Pierre Bourgin, RD10, F-78000 Versailles, France.

³AgroParisTech, Institut Jean-Pierre Bourgin, RD-10, F-78000 Versailles, France.

⁴Department of Cell Biology, National Institute for Basic Biology, Okazaki 444-8585, Japan.

⁵Department of Basic Biology, School of Life Science, The Graduate University for Advanced Studies, Okazaki 444-8585, Japan. ⁶RIKEN Center for Sustainable Resource Science, Tsurumi-ku, Yokohama 230-0045, Japan. ⁷Frontier Research Center, Tokyo Institute of Technology, Yokohama 226-8503, Japan.

*Present address: Department of Applied Biological Chemistry, Faculty of Agriculture, Niigata University, 8050 Ikarashi-2, Niigata 950-2181, Japan.

‡Authors for correspondence (kohki.yoshimoto@versailles.inra.fr; yohsumi@iri.titech.ac.jp)

This is an Open Access article distributed under the terms of the Creative Commons Attribution License (<http://creativecommons.org/licenses/by/3.0>), which permits unrestricted use, distribution and reproduction in any medium provided that the original work is properly attributed.

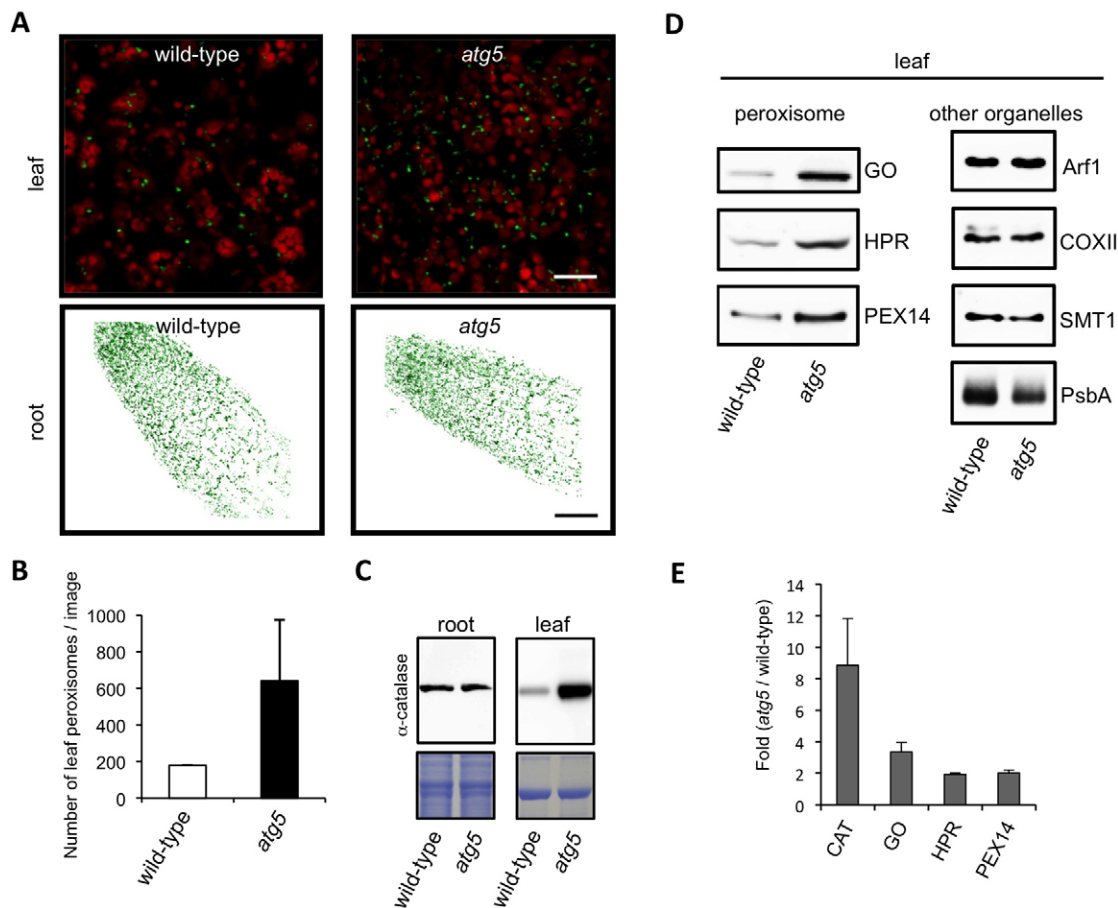


Fig. 1. Autophagy deficiency causes an increase in peroxisomes in leaves. (A) Confocal microscopic images of GFP-PTS1 in wild-type and *atg5* *Arabidopsis*. Green and red signals indicate peroxisomes and chlorophyll autofluorescence, respectively. In root images, projected images of z-stacks are shown. Scale bars: 25 μ m in leaves; 50 μ m in roots. (B) Quantification of the peroxisome number in wild-type and *atg5* leaves. The number of peroxisomes per leaf section was counted. Results are shown as the mean, error bars indicate the s.d. ($n=5$, three independent experiments). (C) Catalase protein levels in wild-type and *atg5* *Arabidopsis*. Total protein samples were subjected to SDS-PAGE and immunoblotting analysis with anti-catalase antibodies. Membranes stained with Coomassie Brilliant Blue are shown in the bottom panels as controls to ensure the loading of equivalent amounts of protein into each lane. (D) Immunoblots showing the protein levels of organelle marker proteins in wild-type and *atg5* leaves. Anti-Arf1, -COXII, -SMT1 and -PsbA antibodies were used as markers for the Golgi apparatus, mitochondria, ER and chloroplast, respectively. Anti-GO, -HPR and -PEX14 antibodies were used as peroxisome markers. (E) Quantification of the protein levels of peroxisomal proteins in leaves. Fold change ratios of peroxisomal protein levels in *atg5* leaves against those in wild-type leaves were calculated using ImageQuant TL software. Each value represents the mean \pm s.d. of at least three independent experiments.

As it has been reported that overexpression of *PEX11* genes, which encode peroxisomal membrane proteins, causes an increase in peroxisome number (Orth et al., 2007), we checked the transcript levels of the *PEX11* genes in *atg* mutants. However, the transcription levels of *PEX11* genes in *atg* mutants were similar to those in wild type (supplementary material Fig. S2B). We further confirmed that peroxisome numbers were increased even in *NahG atg5* plant leaves (supplementary material Fig. S3), in which endogenous salicylic acid (SA) is depleted and consequently the early senescence phenotype is suppressed (Yoshimoto et al., 2009). This indicated that the increase in peroxisome number was not caused by side effects, such as highly accumulated SA or the onset of senescence in *atg* mutants. These results further support the view that peroxisomes in leaves undergo less degradation in *atg* mutants, resulting in an increased number of peroxisomes.

We next examined whether autophagy preferentially degrades only peroxisomes and not other organelles. For this, western blotting analysis was performed using antibodies against representative organelle marker proteins to compare the protein

levels of each organelle between wild-type and *atg5* leaves. As shown in Fig. 1D,E, only peroxisomal proteins were increased in *atg5* leaves. In contrast to the increase in peroxisome number, there was no increase in the number of mitochondria in *atg5* leaves (supplementary material Fig. S4), strongly suggesting that leaf peroxisomes are selectively degraded by autophagy.

Next, the fine structure of peroxisomes in the leaves of *atg* mutants was examined by electron microscopy (EM) (Fig. 2A). Consistent with the results of fluorescence imaging (Fig. 1A, upper-right panel), many peroxisomes were present in *atg* mutants. In addition, we found that many peroxisomes in *atg* mutants contained some electron-dense regions (Fig. 2A, right panel; Fig. 2B; supplementary material Table S1).

As the levels of catalase protein were markedly increased in *atg5* leaves compared to those of other peroxisomal proteins (Fig. 1E), we examined the intracellular states of the highly accumulated catalase by immuno-EM analysis (Fig. 2C). Gold particles conjugated with anti-catalase antibodies were evenly distributed in normal peroxisomes. In abnormal peroxisomes, however, the density of gold particles was markedly elevated in

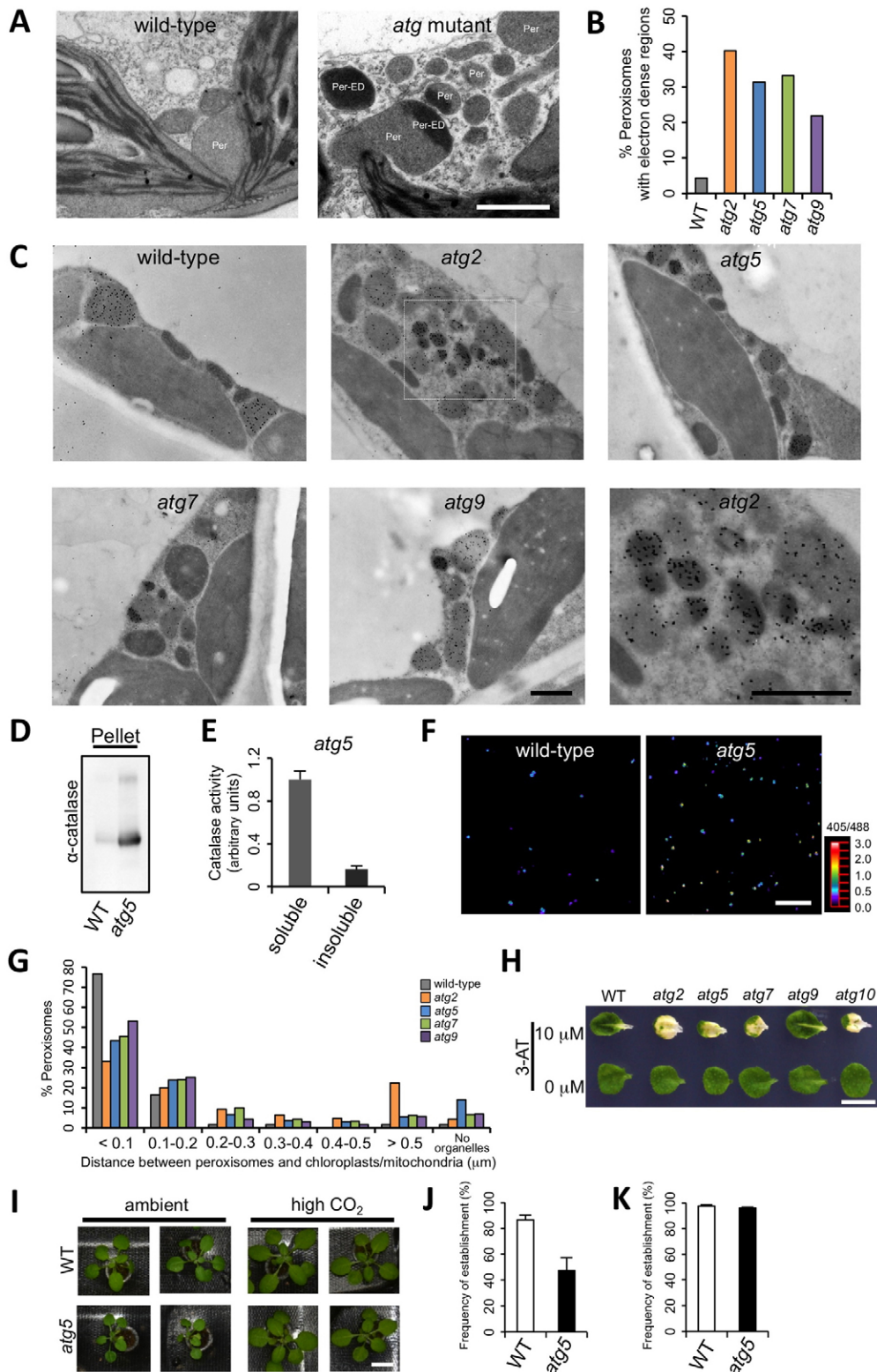


Fig. 2. See next page for legend.

the electron-dense regions and, in such peroxisomes, the density of gold particles was reduced in normal regions, indicating that catalase was concentrated in the electron-dense regions. The electron-dense regions of *atg* mutant peroxisomes had the appearance of structures that have been reported as aggregates

of dysfunctional peroxisome-matrix proteins in the peroxisomal Lon protease-deficient fungus (Bartoszewski et al., 2012). Based on these observations, we hypothesized that the electron-dense regions are dysfunctional protein aggregates, one of the major components of which is catalase. Indeed, there were differences

Fig. 2. Abnormal peroxisomes accumulate in *atg* mutant leaves.

(A) Fine structures of leaf peroxisomes in wild-type and *atg*-mutant *Arabidopsis*. Per, peroxisome; Per-ED, electron-dense region in peroxisome. Scale bar: 1 μ m. (B) The percentage of peroxisomes with electron-dense regions in wild-type and *atg*-mutant leaf peroxisomes. Both normal and abnormal leaf peroxisomes containing electron-dense regions were counted on random EM images and the frequencies were calculated (supplementary material Table S1). (C) Immuno-EM images of wild-type and *atg*-mutant leaf peroxisomes using an antibody against catalase. Black dots represent gold particles labeled with anti-catalase antibody. The white dotted square indicates the enlarged area shown in the lower right panel. Scale bars: 1 μ m. (D) High levels of accumulated insoluble catalase in *atg5*. The pellet samples were subjected to immunoblotting analysis with anti-catalase antibody. (E) The catalase activities in the soluble and insoluble fractions from *atg5* leaves. The activity is expressed in arbitrary units as the mean \pm s.d. of three different experiments. (F) Redox states within peroxisomes in leaves of wild-type and *atg5*. Using redox-sensitive GFP (roGFP2), redox states within peroxisomes in leaves were compared between wild-type and *atg5*. Ratiometric images of the fluorescence excited by 405 and 488 nm lasers are shown. The color scale for the ratio values indicates the reduced state in dark color and the oxidized state in bright color. Scale bar: 10 μ m. (G) Distributions of the distances between peroxisomes and chloroplasts and/or mitochondria. For all peroxisomes or randomly taken EM images the distance from each peroxisome to the nearest chloroplast and/or mitochondrion was measured (supplementary material Table S2) and the percentages at each distance are shown. No organelles, there were no chloroplasts or mitochondria around the peroxisomes. (H) Hypersensitivity of autophagy-defective *Arabidopsis* leaves to catalase inhibitor. Two-week-old seedlings grown on Murashige and Skoog (MS) medium without sucrose (MS-C) were transferred to MS-C with or without 10 μ M 3-aminotriazole (3-AT) for an additional 14 days. The eighth or ninth leaves are shown. Scale bar: 1 cm. (I) The phenotype of *atg5* under high-CO₂ conditions. Seedlings of wild-type and *atg5* were grown hydroponically and supplied with standard nutrients under ambient (360 ppm CO₂) or elevated CO₂ (2000 ppm CO₂) conditions for 3 weeks. Scale bar: 1 cm. (J,K) The frequency of seedling establishment on medium without (J) or with (K) supplemental sugars (1%). Seedling establishment was scored 7 days after germination as the ability to develop true leaves. Error bars indicate the s.d. ($n=60$, three independent experiments).

in the biochemical features of catalase between wild-type and *atg5* leaves; high levels of insoluble catalase were present in *atg5* leaves (Fig. 2D), and its enzyme activity was substantially lower than that of soluble catalase (Fig. 2E), indicating that *atg* mutants accumulated an inactive form(s) of catalase. Furthermore, the redox status of a proportion of peroxisomes in the *atg5* mutant was disturbed, showing a more oxidized state than wild-type ones (Fig. 2F). These results suggest that peroxisomes with electron-dense regions in *atg* mutants are dysfunctional. We also found that peroxisomes in *atg* mutant leaves did not show the appropriate intracellular localization (Fig. 2G). Leaf peroxisomes are usually tightly attached to chloroplasts and/or mitochondria, where they cycle metabolites among these organelles during photorespiration. In wild-type leaves, almost 80% of peroxisomes were located within a distance of 0.1 μ m from chloroplasts and/or mitochondria. In *atg* mutant leaves, however, more than 45% of peroxisomes were separated from these organelles and were often clustered together, which would also lead to a reduction of peroxisomal capability (Prestele et al., 2010). Leaves of *atg* mutants were indeed hypersensitive to the catalase inhibitor 3-aminotriazole (Fig. 2H), even though the levels of catalase protein were increased, and this result closely correlated with the accumulation of inactive form(s) of catalase and the mislocalization of peroxisomes in *atg* mutants.

Consistent with our findings, *atg* mutants showed characteristic phenotypes similar to those observed in peroxisomal-function-defective plants. *Arabidopsis* photorespiratory mutants show

stunted or decelerated growth under standard atmospheric conditions but grow normally in air enriched in CO₂, when photorespiration is suppressed (Reumann and Weber, 2006). Likewise, the decelerated growth phenotype observed in the *atg5* mutant was partially suppressed under high CO₂ conditions (Fig. 2I). We also examined postgerminative seedling establishment on sugar-free medium as an index of peroxisomal ability. As *Arabidopsis* cotyledons catabolize fatty acids into sugars in glyoxysomes, a decline in peroxisomal activity would result in a lower percentage of seedlings developing true leaves on sugar-free medium (Fulda et al., 2004; Rylott et al., 2006). Indeed, the *atg5* mutant showed a lower frequency of seedling development without supplemental sugars. Cotyledons of ~50% of *atg5* seedlings did not fully expand and the production of true leaves was prevented, whereas this was not the case in wild-type seedlings (Fig. 2J). This growth defect in *atg5* was rescued by exogenous application of sugars (Fig. 2K).

The accumulation of abnormal peroxisomes in *atg* mutants prompted us to examine whether autophagy transports peroxisomes to the vacuolar lumen for degradation. For this purpose, an *atg5* transgenic was generated. In this mutant, the autophagic defect can be complemented through induction of *ATG5* gene expression by treatment with 17- β -estradiol, and peroxisomes can be visualized by monitoring GFP fluorescence by confocal fluorescence microscopy. The number of peroxisomes was reduced in the transgenic plants after 17- β -estradiol treatment (Fig. 3A, upper-right panel), whereas control leaves still retained a large number of peroxisomes (Fig. 3A, upper-left panel). To confirm that peroxisomes were delivered into the vacuolar lumen by autophagy, transgenic leaves were incubated in the dark after 17- β -estradiol treatment as GFP fluorescence cannot be detected in the vacuolar lumen in plants that are kept in the light (Tamura et al., 2003). The number of peroxisomes was reduced in 17- β -estradiol-treated leaves, and the vacuolar lumens in these cells contained GFP (Fig. 3A, lower right panel). When plant cells are treated with the V-ATPase inhibitor concanamycin A, autophagic bodies can also be detected inside the vacuolar lumen as small randomly moving vesicles (Yoshimoto et al., 2004). In concanamycin-A-treated cells without 17- β -estradiol treatment, in which autophagy is defective, peroxisomes were detected in the cytoplasm and did not show much movement, sometimes showing rectilinear motion along the cytoskeleton (supplementary material Movie 1). After 17- β -estradiol treatment, however, highly mobile peroxisomes were observed (supplementary material Movie 2), suggesting that peroxisomes were present in autophagic bodies within the vacuole. These results indicate that peroxisomes are delivered to the vacuole by autophagy for degradation.

We then sought to determine the mechanism by which selectivity in the degradation of plant peroxisomes by autophagy is guaranteed. On EM images, some of the peroxisomes in *atg* mutants appeared to be fragmented and consisted only of electron-dense material (Fig. 2A,C). This might explain the marked accumulation of catalases in *atg5* leaves (Fig. 1E). A proportion of peroxisomes containing protein aggregates appeared to be segregated or 'torn off' from the whole peroxisome by unknown mechanisms (Fig. 3B), thus dysfunctional peroxisomal proteins could be selectively degraded by autophagy. In addition, the data for the frequency of peroxisomes with electron-dense regions indicated that the increased number of peroxisomes in *atg* mutants was mainly due to the increase of peroxisomes with electron-dense regions

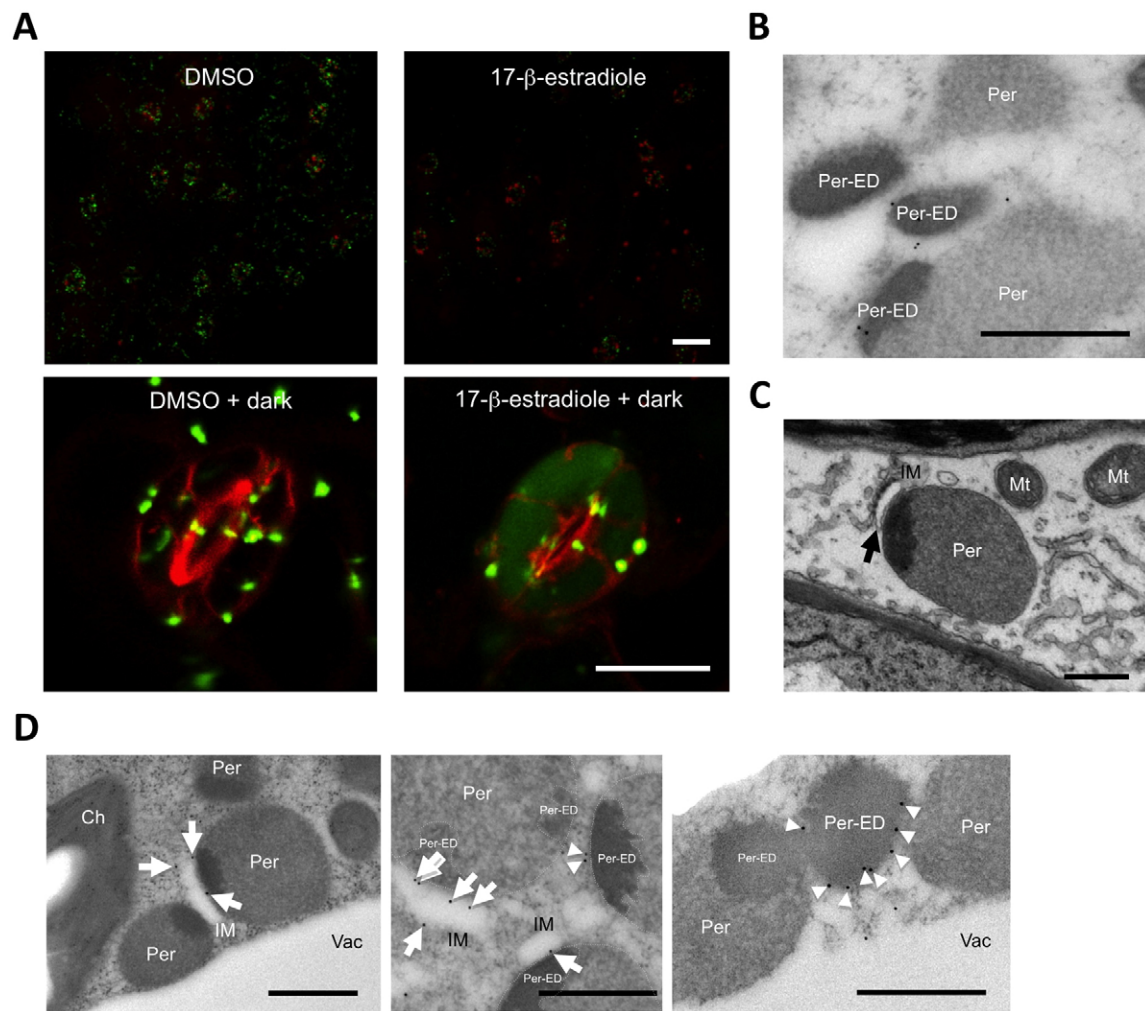


Fig. 3. Peroxisomes are delivered into the vacuolar lumen and are degraded by autophagy for quality control. (A) The behavior of peroxisomes in conditionally complementable *atg5* transgenic leaves. Leaves from the *atg5* transgenic harboring both the *Arabidopsis* ATG5 cDNA driven by an estradiol-inducible promoter and the gene for GFP-PTS1 were incubated with 17- β -estradiol to artificially regulate autophagic ability under light (upper panels) and dark (lower panels) conditions. The green dot signal indicates peroxisomes. The red signal in the upper panels indicates chlorophyll autofluorescence. The red signal in the lower panels indicates vacuolar membranes stained by FM 4-64. Scale bars: 25 μ m, upper panels; 10 μ m, lower panels. (B–D) Immuno-EM (B,D) and conventional EM (C) pictures of *atg2* leaves. Samples for (B,D) were prepared by high-pressure freezing and freeze substitution to observe intracellular fine structures in a state as close as possible to that existing *in vivo*. Electron-lucent membrane structures and gold particles labeled with anti-ATG8a antibodies are indicated by the black arrow (C) and white arrows or arrowheads (D), respectively. Ch, chloroplast; IM, seed of isolation membrane; Mt, mitochondrion; Per, peroxisome; Per-ED, electron-dense region in peroxisome; Vac, vacuole. Scale bars: 500 nm.

(supplementary material Table S1), suggesting that there is selective degradation of abnormal peroxisomes in wild-type leaves. This selectivity was further confirmed by the results of the EM analyses in this study. Examination of the fine structures of peroxisomes in *atg* mutants revealed an electron-lucent membrane structure, which was located adjacent to the endoplasmic reticulum (ER), occasionally present beside peroxisomes in *atg2* leaves (Fig. 3C, black arrow). Surprisingly, these membrane structures were always tightly attached to the sites of the electron-dense regions (supplementary material Table S3). In a yeast *atg2* mutant, many Atg proteins, including Atg8, accumulated at high levels in pre-autophagosomal structures (Suzuki et al., 2007), suggesting that an early autophagic structure called the ‘isolation membrane’ forms in the *atg2* mutant but this mutant cannot complete autophagosome formation. In addition, it has been reported that the ER is one of the sources of isolation membranes in mammalian

cells in culture (Hayashi-Nishino et al., 2009). These observations suggest that the electron-lucent membrane structures could be the seeds of the isolation membranes. In support of this suggestion, immuno-EM analysis using antibodies against *Arabidopsis* ATG8a, which is an autophagosomal membrane marker protein (Yoshimoto et al., 2004; Contento et al., 2005; Thompson et al., 2005), showed that ATG8 was localized on the electron-lucent membrane structures (Fig. 3D, left and middle panel, white arrows). Furthermore, we found that ATG8 was specifically localized on the surface of the electron-dense peroxisome (Fig. 3D, right and middle panel, white arrowheads). This finding is consistent with a previously proposed model of the selective autophagy pathway, in which ATG8 first recognizes a target by direct interaction with an ATG8-family-interacting motif and is then conjugated to phosphatidylethanolamine to recruit and expand the isolation membrane in the proximity of the target (Kuma et al.,

2007; Yamaguchi et al., 2010). Taken together, these observations indicate that dysfunctional peroxisomes must be enwrapped in autophagosomes following the recognition of the sites of electron-dense regions by the machinery responsible for autophagosome formation.

Our results show that autophagy maintains the quality of peroxisomes in an organ-specific manner, which is probably dependent on peroxisomal functions, by the removal of dysfunctional peroxisomes to the vacuole for degradation. Several lines of evidence suggest that *Arabidopsis* has some selective mechanism by which autophagy specifically recognizes dysfunctional peroxisomes. The observation that autophagosomal structures precisely recognize the sites of electron-dense regions, which are most likely aggregates of dysfunctional proteins, is reminiscent of the selective autophagic degradation of damaged mitochondria in mammals (Youle and Narendra, 2011). Thus, the molecular mechanism underlying the selectivity might involve protein–protein interactions between cargo receptor(s) and adaptor(s) and autophagosomal membrane protein(s) (Noda et al., 2010). In plants, the peroxisomal membrane can also be heavily damaged by ROS produced by peroxisomal oxidative reactions during the life cycle. Therefore, damaged membranes might be recognized by peroxisomal-membrane-localized receptor and adaptor protein(s). In mammalian cells, it has been proposed that the recognition of ubiquitinated peroxisomal membrane proteins by p62 (SQSTM1) and/or its homolog NBR1 (next to BRCA1 gene 1) confers selectivity for peroxisome degradation by autophagy (Kim et al., 2008; Deosaran et al., 2013). Although plant NBR1, which possesses hybrid properties of mammalian NBR1 and p62, has been identified (Svenning et al., 2011; Zientara-Rytter et al., 2011), it is still not known whether it has a role in pexophagy in plants. Because our western blot analysis using isolated leaf peroxisomes does not show a substantial increase in ubiquitinated proteins in *atg2* peroxisomes (data not shown), and immuno-EM analysis using anti-ubiquitin antibodies does not show ubiquitinylation of peroxisomal membrane proteins near the electron-dense regions (data not shown), the mechanism of selective peroxisome degradation in plants might be different from that in mammals. In addition, pexophagy must have plant-specific physiological significance. Through selective elimination of dysfunctional peroxisomes during peroxisomal oxidation processes, autophagy appears to play crucial roles in the early development of oilseed plants and the maintenance of photosynthetic function. Only plants, which are sessile and photosynthetic organisms, would have evolved this type of pexophagy as a unique strategy to survive conditions of severe environmental stress.

MATERIALS AND METHODS

Plant materials and growth conditions

Arabidopsis thaliana ecotype Columbia was used in this study. The seeds of transfer (T)-DNA knockout mutants of *ATG2*, *ATG5*, *ATG7*, *ATG9* and *ATG10* [*atg2-1* (SALK_076727), *atg5-1* (SAIL_129B07), *atg7-2* (GABI_655B06), *atg9-3* (SALK_130796) and *atg10-1* (SALK_084434), respectively] were obtained from either the Nottingham *Arabidopsis* Resource Center or GABI-Kat. For high-CO₂ conditions, plants were grown hydroponically under 2000 ppm CO₂ adjusted in an open gas-exchange system including phytochambers at 22°C with 65–80% relative humidity and a 12-h photoperiod.

Fluorescence microscopy

To visualize peroxisomes in *atg* mutants, *Arabidopsis* carrying a transgene encoding green fluorescent protein (GFP) fused with a

peroxisomal targeting signal (GFP–PTS1) (Mano et al., 2002) was crossed to *atg2*, *atg5* and *atg7* mutants. To obtain *NahG atg5* mutants expressing GFP–PTS1, *atg5* GFP–PTS1 was crossed with *NahG atg5* plants. GFP fusion proteins were visualized using a Zeiss LSM 510 confocal laser scanning microscope (Zeiss, Jena, Germany) as described previously (Yoshimoto et al., 2004). To visualize mitochondria and vacuolar membranes, *Arabidopsis* leaves were stained with MitoTracker Green (MTG; Invitrogen, Carlsbad, CA) and FM 4-64 (Invitrogen), respectively, then observed by confocal microscopy with a 488 nm laser for MTG observation (emission 495–535 nm) and a 514 nm laser for FM 4-64 observation (emission 615–645 nm). Real-time movies were taken with a fluorescence microscope (BX51; Olympus, Tokyo, Japan) equipped with a CCD camera (DP72; Olympus).

Immunoblotting analysis

Four-week-old plants were used for immunoblotting analyses. Plant total protein samples were prepared as described previously (Yoshimoto et al., 2004), except in the case of immunoblotting analysis using the pellet fraction (Fig. 2D), for which protein extracts homogenized with 100 mM Tris-HCl pH 8.0, 20% glycerol and 30 mM dithiothreitol (DTT) were centrifuged at 17,750 *g* for 15 min, and the resultant pellet fraction was used. Aliquots of 1 or 5 µg of protein were subjected to immunoblotting analysis using anti-catalase (Yamaguchi and Nishimura, 1984), anti-glycolate oxidase (GO; Tsugeki et al., 1993) or anti-hydroxypyruvate reductase (HPR; Mano et al., 1997), anti-peroxisomal membrane protein 14 (PEX14), anti-ADP ribosylation factor 1 (Arf1), anti-cytochrome *c* oxidase subunit 2 (COXII), anti-sterol methyltransferase 1 (SMT1) and anti-D1 protein of photosystem II (PsbA) antibodies (Agrisera, Vännäs, Sweden).

Electron microscopy

Non-senescent leaves from 4-week-old *Arabidopsis* plants grown under nutrient-sufficient conditions were used. Transmission electron microscopy (TEM) (Fig. 2A; Fig. 3C) was performed according to a previous study (Toyooka et al., 2000) with some modifications. The ultrathin sections were examined by TEM (JEM-1400; JEOL Ltd, Tokyo, Japan) at 80 kV. Immunoelectron microscopy using anti-catalase antibody (Yamaguchi and Nishimura, 1984) (Fig. 2C) was performed as described previously (Nishimura et al., 1993), except for the antibody dilution (1:5000). Immunoelectron microscopy using anti-ATG8a antibody (ab77003; Abcam, Cambridge, UK) (Fig. 3D) or anti-polyubiquitin 11 (UBQ11) antibody (AS08 307; Agrisera, Vännäs, Sweden) (data not shown) was performed according to a previous study (Toyooka et al., 2009), with some modifications. *Arabidopsis* leaves were frozen in a high-pressure freezing machine (Leica EM PACT; Leica Microsystems GmbH). The sections were labeled with antibodies (1:10) in Tris-buffered saline (TBS) at 4°C overnight.

Catalase activity measurements

Leaf samples were taken from approximately the same position of the respective leaf and were homogenized on ice in a buffer consisting of 100 mM Tris-HCl pH 8.0, 20% glycerol and 30 mM DTT. The homogenates were centrifuged at 17,750 *g* for 15 min to generate supernatants and pellets. The resulting supernatant samples and pellet samples that were rinsed twice with protein extraction buffer were subjected to measurement of catalase activities spectrophotometrically, by monitoring the changes of H₂O₂ at OD₂₄₀ at room temperature as described previously (Durner and Klessig, 1996). The catalase activities in soluble and insoluble fractions were normalized to the protein levels of catalase, which were determined by immunoblotting analysis using anti-catalase antibodies.

Comparison of redox state within peroxisomes

To compare the redox state within peroxisomes between wild type and *atg5*, we generated transgenic wild-type and *atg5* plants expressing redox-sensitive GFP (roGFP2) fused with PTS1 under the control of the cauliflower mosaic virus (CaMV) 35S promoter. The leaves were observed by confocal microscopy. roGFP2 was excited with 405 and 488 nm lasers and the fluorescence was measured with a band pass filter

of 505–530 nm. Then ratiometric images of 405:488 were generated as described previously (Meyer et al., 2007).

Construction of the estradiol-inducible complementation system

The *ATG5* coding region (nucleotides 1–1014) was amplified by PCR from full-length cDNA using the primers 5'-TCCCCCGGGAT-GGCGAAGGAAGCGG-3' and 5'-GCTCTAGATCACCTTTGAGGA-GCTTTC-3'. The resulting PCR product was inserted into the *EcoRV* site of the pBluescript II vector and the resulting plasmid was designated as pH52. To construct a plasmid for generating stable transformants expressing *ATG5* cDNA driven by the estradiol-inducible promoter, pH52 was digested with *ApaI* and *SpeI* and was ligated into the same sites of pER8 (Zuo et al., 2006). The construct was verified by sequencing and was introduced into *atg5-1 Arabidopsis* plants by the floral-dip method of *in planta Agrobacterium-tumefaciens*-mediated transformation (Clough and Bent, 1998). Chemical treatments were carried out both by injections using a syringe without needle and by submerging tissue in liquid medium containing 10 μ M 17- β -estradiol (Sigma, St Louis, MO).

RT-PCR

RT-PCR for catalase genes and peroxisome division and proliferation-related genes, *PEX11a-11e*, was performed as described previously (Yoshimoto et al., 2004). cDNA derived from 0.2 μ g of total RNA was used as the template for PCR. The gene-specific primers used are described in supplementary material Table S4.

Acknowledgements

The authors would like to thank Ivana Saska for critical reading of the manuscript. The pER8 plasmid was a kind gift from Nam-Hai Chua of Rockefeller University. We also thank Mayumi Wakazaki of RIKEN for technical assistance on the EM analyses and Kazuo Tsugane of the National Institute for Basic Biology for expert care of our plants in the high-CO₂ experiment. The high-CO₂ experiment was supported by the Japan Advanced Plant Science Network.

Competing interests

The authors declare no competing interests.

Author contributions

K.Y. designed the research. M.K., M.S. and K.T. performed electron microscopic observations. K.Y. performed other experiments. K.Y., M.S., M.K., K.O., M.S., K.T., K.S., M.N. and Y.O. analyzed the data and contributed to data interpretation and the preparation of the manuscript. K.Y. and Y.O. wrote the manuscript.

Funding

This research was funded in part by a research fellowship from the RIKEN Special Postdoctoral Researchers Program [grant number 19-062 to K.Y.]; by Grant-in-Aid for Young Scientists (B) [grant number 22770049 to K.Y.]; and by the Institut National de la Recherche Agronomique (INRA) Package Program from INRA, France. Deposited in PMC for immediate release.

Supplementary material

Supplementary material available online at <http://jcs.biologists.org/lookup/suppl/doi:10.1242/jcs.139709/-DC1>

References

- Asakura, M., Ninomiya, S., Sugimoto, M., Oku, M., Yamashita, S., Okuno, T., Sakai, Y. and Takano, Y. (2009). Atg26-mediated pexophagy is required for host invasion by the plant pathogenic fungus *Colletotrichum orbiculare*. *Plant Cell* **21**, 1291–1304.
- Bartoszewski, M., Williams, C., Kikhney, A., Opaliński, L., van Roermund, C. W., de Boer, R., Veenhuis, M. and van der Klei, I. J. (2012). Peroxisomal proteostasis involves a Lon family protein that functions as protease and chaperone. *J. Biol. Chem.* **287**, 27380–27395.
- Beevers, H. (1979). Microbodies in higher plants. *Annu. Rev. Plant Physiol.* **30**, 159–193.
- Clough, S. J. and Bent, A. F. (1998). Floral dip: a simplified method for *Agrobacterium*-mediated transformation of *Arabidopsis thaliana*. *Plant J.* **16**, 735–743.
- Contento, A. L., Xiong, Y. and Bassham, D. C. (2005). Visualization of autophagy in *Arabidopsis* using the fluorescent dye monodansylcadaverine and a GFP-AtATG8e fusion protein. *Plant J.* **42**, 598–608.
- De Duve, C. and Baudhuin, P. (1966). Peroxisomes (microbodies and related particles). *Physiol. Rev.* **46**, 323–357.
- del Río, L. A., Sandalio, L. M., Corpas, F. J., Palma, J. M. and Barroso, J. B. (2006). Reactive oxygen species and reactive nitrogen species in peroxisomes. Production, scavenging, and role in cell signaling. *Plant Physiol.* **141**, 330–335.
- Deosaran, E., Larsen, K. B., Hua, R., Sargent, G., Wang, Y., Kim, S., Lamark, T., Jauregui, M., Law, K., Lippincott-Schwartz, J. et al. (2013). NBR1 acts as an autophagy receptor for peroxisomes. *J. Cell Sci.* **126**, 939–952.
- Durner, J. and Klessig, D. F. (1996). Salicylic acid is a modulator of tobacco and mammalian catalases. *J. Biol. Chem.* **271**, 28492–28501.
- Foyer, C. H. and Noctor, G. (2003). Redox sensing and signalling associated with reactive oxygen in chloroplasts, peroxisomes and mitochondria. *Physiol. Plant.* **119**, 355–364.
- Frugoli, J. A., Zhong, H. H., Nuccio, M. L., McCourt, P., McPeck, M. A., Thomas, T. L. and McClung, C. R. (1996). Catalase is encoded by a multigene family in *Arabidopsis thaliana* (L.) Heynh. *Plant Physiol.* **112**, 327–336.
- Fulda, M., Schnurr, J., Abbadi, A., Heinz, E. and Browse, J. (2004). Peroxisomal Acyl-CoA synthetase activity is essential for seedling development in *Arabidopsis thaliana*. *Plant Cell* **16**, 394–405.
- Hayashi-Nishino, M., Fujita, N., Noda, T., Yamaguchi, A., Yoshimori, T. and Yamamoto, A. (2009). A subdomain of the endoplasmic reticulum forms a cradle for autophagosome formation. *Nat. Cell Biol.* **11**, 1433–1437.
- Iwata, J., Ezaki, J., Komatsu, M., Yokota, S., Ueno, T., Tanida, I., Chiba, T., Tanaka, K. and Kominami, E. (2006). Excess peroxisomes are degraded by autophagic machinery in mammals. *J. Biol. Chem.* **281**, 4035–4041.
- Kim, P. K., Hailey, D. W., Mullen, R. T. and Lippincott-Schwartz, J. (2008). Ubiquitin signals autophagic degradation of cytosolic proteins and peroxisomes. *Proc. Natl. Acad. Sci. USA* **105**, 20567–20574.
- Kuma, A., Matsui, M. and Mizushima, N. (2007). LC3, an autophagosome marker, can be incorporated into protein aggregates independent of autophagy: caution in the interpretation of LC3 localization. *Autophagy* **3**, 323–328.
- Mano, S., Hayashi, M., Kondo, M. and Nishimura, M. (1997). Hydroxypyruvate reductase with a carboxy-terminal targeting signal to microbodies is expressed in *Arabidopsis*. *Plant Cell Physiol.* **38**, 449–455.
- Mano, S., Nakamori, C., Hayashi, M., Kato, A., Kondo, M. and Nishimura, M. (2002). Distribution and characterization of peroxisomes in *Arabidopsis* by visualization with GFP: dynamic morphology and actin-dependent movement. *Plant Cell Physiol.* **43**, 331–341.
- Meyer, A. J., Brach, T., Marty, L., Kreye, S., Rouhier, N., Jacquot, J.-P. and Hell, R. (2007). Redox-sensitive GFP in *Arabidopsis thaliana* is a quantitative biosensor for the redox potential of the cellular glutathione redox buffer. *Plant J.* **52**, 973–986.
- Mizushima, N., Yoshimori, T. and Ohsumi, Y. (2011). The role of Atg proteins in autophagosome formation. *Annu. Rev. Cell Dev. Biol.* **27**, 107–132.
- Nishimura, M., Takeuchi, Y., Bellis, L. and Hara-Nishimura, I. (1993). Leaf peroxisomes are directly transformed to glyoxysomes during senescence of pumpkin cotyledons. *Protoplasma* **175**, 131–137.
- Noda, N. N., Ohsumi, Y. and Inagaki, F. (2010). Atg8-family interacting motif crucial for selective autophagy. *FEBS Lett.* **584**, 1379–1385.
- Orth, T., Reumann, S., Zhang, X., Fan, J., Wenzel, D., Quan, S. and Hu, J. (2007). The PEROXIN11 protein family controls peroxisome proliferation in *Arabidopsis*. *Plant Cell* **19**, 333–350.
- Prestele, J., Hierl, G., Scherling, C., Hetkamp, S., Schwechheimer, C., Isono, E., Weckwerth, W., Wanner, G. and Gietl, C. (2010). Different functions of the C₂HC₄ zinc RING finger peroxins PEX10, PEX2, and PEX12 in peroxisome formation and matrix protein import. *Proc. Natl. Acad. Sci. USA* **107**, 14915–14920.
- Reumann, S. and Weber, A. P. (2006). Plant peroxisomes respire in the light: some gaps of the photorespiratory C₂ cycle have become filled – others remain. *Biochim. Biophys. Acta* **1763**, 1496–1510.
- Rylott, E. L., Eastmond, P. J., Gilday, A. D., Slocombe, S. P., Larson, T. R., Baker, A. and Graham, I. A. (2006). The *Arabidopsis thaliana* multifunctional protein gene (MFP2) of peroxisomal β -oxidation is essential for seedling establishment. *Plant J.* **45**, 930–941.
- Sakai, Y., Oku, M., van der Klei, I. J. and Kiel, J. A. (2006). Pexophagy: autophagic degradation of peroxisomes. *Biochim. Biophys. Acta* **1763**, 1767–1775.
- Suzuki, K., Kubota, Y., Sekito, T. and Ohsumi, Y. (2007). Hierarchy of Atg proteins in pre-autophagosomal structure organization. *Genes Cells* **12**, 209–218.
- Svenning, S., Lamark, T., Krause, K. and Johansen, T. (2011). Plant NBR1 is a selective autophagy substrate and a functional hybrid of the mammalian autophagic adaptors NBR1 and p62/SQSTM1. *Autophagy* **7**, 993–1010.
- Tamura, K., Shimada, T., Ono, E., Tanaka, Y., Nagatani, A., Higashi, S. I., Watanabe, M., Nishimura, M. and Hara-Nishimura, I. (2003). Why green fluorescent fusion proteins have not been observed in the vacuoles of higher plants. *Plant J.* **35**, 545–555.
- Thompson, A. R., Doelling, J. H., Suttangkakul, A. and Vierstra, R. D. (2005). Autophagic nutrient recycling in *Arabidopsis* directed by the ATG8 and ATG12 conjugation pathways. *Plant Physiol.* **138**, 2097–2110.
- Toyooka, K., Okamoto, T. and Minamikawa, T. (2000). Mass transport of proform of a KDEL-tailed cysteine proteinase (SH-EP) to protein storage vacuoles by endoplasmic reticulum-derived vesicle is involved in protein mobilization in germinating seeds. *J. Cell Biol.* **148**, 453–464.
- Toyooka, K., Goto, Y., Asatsuma, S., Koizumi, M., Mitsui, T. and Matsuoka, K. (2009). A mobile secretory vesicle cluster involved in mass transport from the Golgi to the plant cell exterior. *Plant Cell* **21**, 1212–1229.

- Tsugeki, R., Hara-Nishimura, I., Mori, H. and Nishimura, M.** (1993). Cloning and sequencing of cDNA for glycolate oxidase from pumpkin cotyledons and northern blot analysis. *Plant Cell Physiol.* **34**, 51-57.
- Yamaguchi, J. and Nishimura, M.** (1984). Purification of glyoxysomal catalase and immunochemical comparison of glyoxysomal and leaf peroxisomal catalase in germinating pumpkin cotyledons. *Plant Physiol.* **74**, 261-267.
- Yamaguchi, M., Noda, N. N., Nakatogawa, H., Kumeta, H., Ohsumi, Y. and Inagaki, F.** (2010). Autophagy-related protein 8 (Atg8) family interacting motif in Atg3 mediates the Atg3-Atg8 interaction and is crucial for the cytoplasm-to-vacuole targeting pathway. *J. Biol. Chem.* **285**, 29599-29607.
- Yoshimoto, K., Hanaoka, H., Sato, S., Kato, T., Tabata, S., Noda, T. and Ohsumi, Y.** (2004). Processing of ATG8s, ubiquitin-like proteins, and their deconjugation by ATG4s are essential for plant autophagy. *Plant Cell* **16**, 2967-2983.
- Yoshimoto, K., Jikumaru, Y., Kamiya, Y., Kusano, M., Consonni, C., Panstruga, R., Ohsumi, Y. and Shirasu, K.** (2009). Autophagy negatively regulates cell death by controlling NPR1-dependent salicylic acid signaling during senescence and the innate immune response in *Arabidopsis*. *Plant Cell* **21**, 2914-2927.
- Youle, R. J. and Narendra, D. P.** (2011). Mechanisms of mitophagy. *Nat. Rev. Mol. Cell Biol.* **12**, 9-14.
- Zientara-Rytter, K., Łukomska, J., Moniuszko, G., Gwozdecki, R., Surowiecki, P., Lewandowska, M., Liszewska, F., Wawrzyńska, A. and Sirko, A.** (2011). Identification and functional analysis of Joka2, a tobacco member of the family of selective autophagy cargo receptors. *Autophagy* **7**, 1145-1158.
- Zuo, J., Hare, P. D. and Chua, N. H.** (2006). Applications of chemical-inducible expression systems in functional genomics and biotechnology. *Methods Mol. Biol.* **323**, 329-342.